

## Optical transitions in $\text{CeSn}_3$ and $\text{LaSn}_3$

This article has been downloaded from IOPscience. Please scroll down to see the full text article.

1992 J. Phys.: Condens. Matter 4 8039

(<http://iopscience.iop.org/0953-8984/4/40/017>)

View [the table of contents for this issue](#), or go to the [journal homepage](#) for more

Download details:

IP Address: 171.66.16.96

The article was downloaded on 11/05/2010 at 00:39

Please note that [terms and conditions apply](#).

## Optical transitions in CeSn<sub>3</sub> and LaSn<sub>3</sub>

Kwang Joo Kim

Department of Physics, Kon-Kuk University, Seoul 133-701, South Korea

Received 16 April 1992

**Abstract.** Interband optical transitions in CeSn<sub>3</sub> and LaSn<sub>3</sub> have been investigated by measuring and calculating from band theory the optical conductivities of both compounds. For both compounds, interband transitions start at low energies (0.3 eV for CeSn<sub>3</sub> and 0.5 eV for LaSn<sub>3</sub>) and these structures are mostly due to d → f and f → d transitions between band-like d and f states originating from Ce or La atoms. The structures at higher energies (greater than 1 eV) strongly involve f → d and d → p transitions with p states originating from Sn atoms. Good qualitative agreement between calculation and experiment has been achieved for these higher-energy structures for both compounds. The larger strength of the structures in CeSn<sub>3</sub> above 1 eV is mainly due to the existence of more occupied band-like f states in CeSn<sub>3</sub> than in LaSn<sub>3</sub>.

### 1. Introduction

The electronic structure of Ce-based systems has been studied extensively in recent years because of the unusual transport and magnetic properties associated with the interactions of the 4f electrons with the electronic environment. The 4f states of Ce in some Ce-based materials are located close to the Fermi level  $E_F$  and have somewhat more extended wavefunctions than those of heavier rare-earth elements in which the 4f states are spatially located deep within the ionic cores, preserving well their atomic character which is dominated by strong intra-atomic Coulomb correlations. A possible interaction of the 4f states with the environment is provided by hybridization of these states with valence band states, which gives a partial band-like character to the 4f electrons. If the 4f states can be treated as being very weakly perturbed by the valence electrons, then the valence bands do not contain much 4f character and the Ce ions can be thought of as having a definite integral valence. Many of the Ce-based materials do not fit into this localized picture and show valence fluctuation (or mixed valency) to some extent. In most of the Ce-based valence-fluctuating systems the ground state has been described as an intermediate-valence (or homogeneous mixed-valence) state where each Ce ion has the same non-integer valence owing to the near degeneracy in energy of the two configurations Ce<sup>3+</sup> 4f<sup>1</sup>, with one core-like f electron, and Ce<sup>4+</sup> 4f<sup>0</sup>, with no core-like f electron [1]. The coexistence of these two configurations gives rise to an intermediate-valence state,  $\Psi = a|4f^1\rangle + b|4f^0\rangle$  with  $|a|^2 + |b|^2 = 1$ . Hence, the theoretical problem is one of describing simultaneously atomic-like configurations, extended band-like states and sometimes transitions between them. There has been a large number of theoretical studies on the Ce-based systems over decades and it is generally accepted that the band theory is applicable to some of the Ce-based systems in which 4f states hybridize

strongly with the valence band states. For localized 4f systems the band theory is still useful to apply because it can give a detailed and not unreasonable physical picture of the electronic interactions as well as a good starting point for estimating the correlation and other effects in the systems.

CeSn<sub>3</sub> is known to be one of the intermediate-valence systems in which the band theory has been applied to explain the electronic properties [2–6]. The electronic specific heat coefficient and the cyclotron effective masses are much larger than those of LaSn<sub>3</sub> [4, 7], the isostructural non-mixed-valence reference material to CeSn<sub>3</sub> without 4f electrons. The magnetic susceptibility of CeSn<sub>3</sub> follows a Curie–Weiss law at high temperatures. It is approximately constant in the 40–300 K region and increases rapidly with decreasing temperature below 40 K [8]. It shows no magnetic ordering down to 1.6 K according to a Mössbauer measurement [9]. On the other hand, the magnetic susceptibility of LaSn<sub>3</sub> follows a Curie–Weiss law above 100 K although there is no evidence for local moments. The susceptibility is approximately constant below 100 K [10]. LaSn<sub>3</sub> also has a relatively high superconducting transition temperature ( $T_c = 6.42$  K). A detailed understanding of the physical properties of LaSn<sub>3</sub> can be helpful in assessing the origin of the anomalous properties of its isostructural mixed-valence compound CeSn<sub>3</sub> which are believed to be due to its one 4f electron.

In the following, we report measurements of the optical conductivities of both CeSn<sub>3</sub> and LaSn<sub>3</sub>. We interpret these spectra by carrying out a band calculation for each material, from which the interband optical conductivity, including electric dipole matrix elements, was calculated. Despite the known shortcomings of treating the 4f states as band-like, we find rather good qualitative agreement between theory and experiment, and that the dominant transitions involve the 4f states via rather strong hybridization with lanthanide 5d states and Sn 5p states in the bands. Thus transitions between the 4f and 5d states account for a major part of the oscillator strength in the 1–4 eV region for both materials, with the conductivity of CeSn<sub>3</sub> being higher because it has more of these types of transition.

Optical measurements on some other Ce and La-based materials have been performed to obtain the dielectric functions either from Kramers–Kronig analyses of the reflectance [11–13] or from ellipsometry [14]. In [12], a comparison is made of the optical spectra of CeCu<sub>6</sub> and LaCu<sub>6</sub>, where a large difference in the optical conductivities was found in the low-energy region (less than 1 eV) where there was little difference in the 1–5 eV region because of the dominance of transitions from the Cu 3d states. In particular, in [14] the optical spectra of CeB<sub>6</sub> and LaB<sub>6</sub> are compared but the conclusions on the role of the 4f electron differ from ours, even though the data are similar to ours for CeSn<sub>3</sub> and LaSn<sub>3</sub>.

## 2. Experimental details

A scanning photometric rotating-analyser–polarizer ellipsometer [15] was used to determine the optical conductivities of the compounds at room temperature. Measurements were made in the 1.5–4.35 eV range at energy intervals of 0.02 eV. The light source was a 150 W Xe-arc lamp. A GM 252 0.25 m grating monochromator, with a spectral dispersion of 3.3 nm mm<sup>-1</sup> grating blazed at 240 nm, was used to produce monochromatic light. A fused SiO<sub>2</sub> quarter-wave retarder was used to reduce the polarization effect of the monochromator. A photomultiplier with an S20 cathode

with a 1.5–5.5 eV range was used as a detector. Both the  $CeSn_3$  and the  $LaSn_3$  samples were single crystals oriented to the (111) and (100) surfaces respectively. Before the measurements, the samples were mechanically polished with abrasives, the final grade being an alumina paste of 0.05  $\mu\text{m}$  particle diameter, and subsequently cleaned by acetone and methanol. These samples oxidize very quickly; so, just after polishing, they were put into a vacuum chamber with a base pressure of  $1 \times 10^{-10}$  Torr and measured. It is expected that the samples are covered with an oxide layer of unknown thickness because of their reactive nature which is stronger for  $LaSn_3$  than for  $CeSn_3$ . To test the effect of the oxide layer, we performed other runs in which the samples were held in air for a more extended period of time before being placed under vacuum. Such treatment produced a lower value of the optical conductivity than that reported here, but only by about 10%. The effect of the Pyrex windows attached to the vacuum chamber in measuring the optical parameters was found to be negligible in the energy range 1.5–4.5 eV by measuring an Au film with and without the windows, which produced identical results.

### 3. Analyses and discussion

A linearized-augmented-plane-wave band calculation for  $CeSn_3$  was carried out in which the 4f states of Ce were treated as valence states, essentially the same as for  $LaSn_3$  which is used as a reference material without an occupied 4f electron. Both compounds crystallize in the  $Cu_3Au$  structure and have nearly the same lattice parameters (4.72  $\text{\AA}$  for  $CeSn_3$  and 4.76  $\text{\AA}$  for  $LaSn_3$ ). The self-consistent crystal potentials for both compounds were taken from the work of Koelling [2] and were constructed using the warped-muffin-tin approximation, which allows the interstitial potential to vary rather than to remain constant. The calculations were scalar relativistic [16] in which the Dirac equation is reduced to omit initially the spin-orbit interaction (but retaining all other relativistic kinematic effects). The spin-orbit interaction was added perturbatively after the semirelativistic bands and wavefunctions had been obtained.

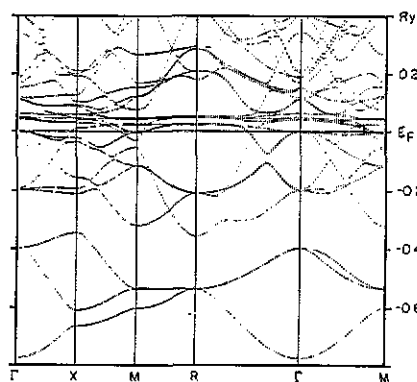


Figure 1. Energy band structure including spin-orbit coupling of  $CeSn_3$  along some high-symmetry directions.

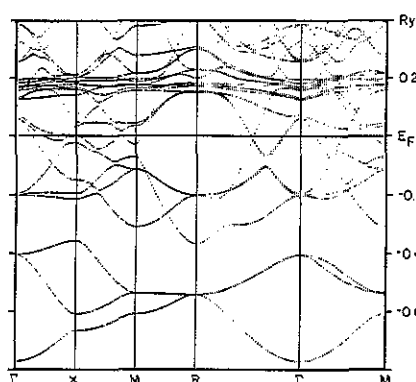


Figure 2. Energy band structure including spin-orbit coupling of  $LaSn_3$  along some high-symmetry directions.

Figures 1 and 2 show the band structures of  $\text{CeSn}_3$  and  $\text{LaSn}_3$  along some high-symmetry directions. Below  $E_F$  the band orderings and separations for both compounds are very similar. The 4f bands of  $\text{CeSn}_3$  are located closer to  $E_F$  and are narrower than those of  $\text{LaSn}_3$ . These band structures including 4f bands could well explain the measured Fermi surface topology for both compounds [2, 6]. For  $\text{CeSn}_3$  the 4f states are concentrated near  $E_F$ , which causes a heavier effective mass and resultant larger electronic specific heat coefficient than for  $\text{LaSn}_3$ , which agrees qualitatively with the experimental results [17]. The existence of the unoccupied 4f states near  $E_F$  for  $\text{CeSn}_3$  and  $\text{CePd}_3$  was detected by bremsstrahlung isochromat spectroscopy measurements [18] while no structure was detected for  $\text{LaPd}_3$  near  $E_F$  [19].

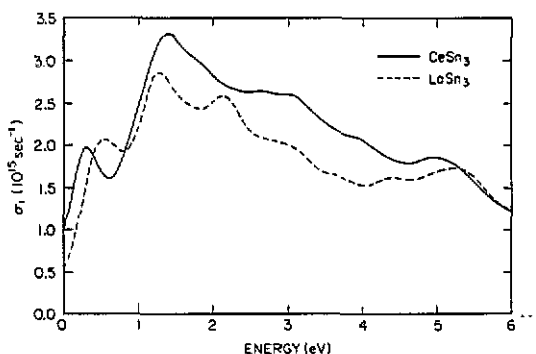


Figure 3. Real part of the complex interband optical conductivities of  $\text{CeSn}_3$  and  $\text{LaSn}_3$  calculated from band structures.

Figure 3 shows the interband optical conductivities of  $\text{CeSn}_3$  and  $\text{LaSn}_3$  calculated using the linear-energy-tetrahedron method [20], in which the energy eigenvalues were evaluated at the four corners of 286 elementary tetrahedra in the irreducible one forty-eighth of the simple-cubic Brillouin zone. The electric dipole matrix elements were calculated using the wavefunctions at the centres of the tetrahedra and were assumed to be constant within a tetrahedron [21]. For both compounds, interband transitions start at low energies (0.3 eV for  $\text{CeSn}_3$  and 0.5 eV for  $\text{LaSn}_3$ ). These structures are caused by  $d \rightarrow f$  and  $f \rightarrow d$  transitions between d and f states originating from Ce or La atoms. According to the band calculation results on  $\text{CePd}_3$  and  $\text{LaPd}_3$ , an interband structure in the optical conductivity was found for  $\text{CePd}_3$  at about the same energy as for  $\text{CeSn}_3$  while no low-energy structure was found for  $\text{LaPd}_3$  [22]. Similar low-energy structures have been found in the experimental spectra of  $\text{CeSb}$  and  $\text{LaSb}$  [13].

Band calculation results for  $\text{CeSn}_3$  and  $\text{LaSn}_3$  also show that the lanthanide 5d character of Ce and La is quite spread in energy across  $E_F$  with a band width of about 10 eV. The 5d states in the rare-earth elements have a larger charge density near the core region than do the other valence states (e.g. 6s) so that they overlap more strongly with the 4f states. In  $\text{LaSn}_3$ , states near  $E_F$  have La 4f and 5d character mixed with considerable Sn p character (f-d-p hybrid states). The electric dipole matrix elements between La 5d-like states near the bottom of the d bands and f-d-p hybrid states above  $E_F$  are rather large, and the joint density of states is also high. These transitions dominate the interband conductivity of  $\text{LaSn}_3$  throughout our spectral region and give rise to the structures at about 1.3, 2.1 and 3 eV. For  $\text{CeSn}_3$

there exists even more 4f character in the states near  $E_F$  than for  $LaSn_3$ . Moreover, f-d-p hybrid states occur both below and above  $E_F$ , allowing them to be both initial and final states for optical transitions. The electric dipole matrix elements and joint density of states are both large, the former larger than for  $LaSn_3$ , and transitions from filled Ce 5d states to empty f-d-p hybrid states and from filled f-d-p hybrid states to empty 5d states cause essentially all the structures in the interband optical conductivity (1.4, 2 and 3 eV) in our spectral region. The large increase in the magnitude of the conductivity of  $CeSn_3$  over that of  $LaSn_3$  arises from the greater mixing of lanthanide 4f states into states near  $E_F$ , giving larger electric dipole matrix elements.

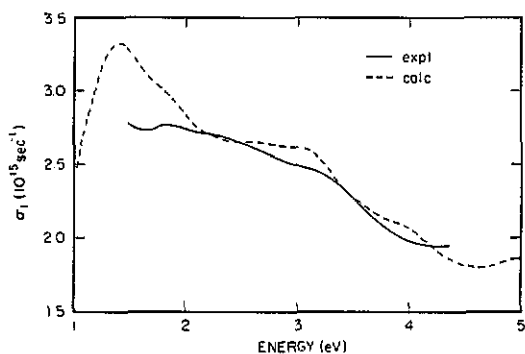


Figure 4. Comparison between the theoretical and experimental results for the optical conductivity of  $CeSn_3$ . No Drude term has been subtracted from the experimental conductivity.

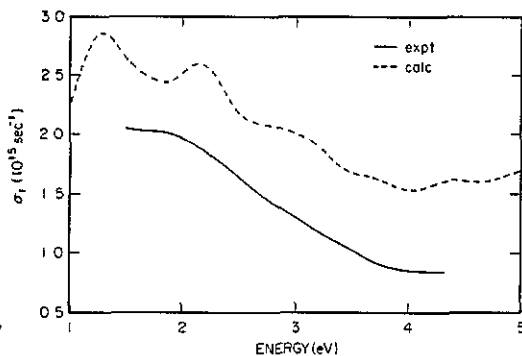


Figure 5. Comparison between the theoretical and experimental results for the optical conductivity of  $LaSn_3$ . No Drude term has been subtracted from the experimental conductivity.

Figures 4 and 5 exhibit comparisons between the calculated optical conductivities and the experimental spectra for both compounds. It is seen that qualitative agreement has been achieved for both compounds. In the case of  $LaSn_3$  the disagreement in magnitude is probably due to faster oxidation for  $LaSn_3$  than for  $CeSn_3$ , causing a reduction in the magnitude of the conductivity. In the experimental spectra,  $LaSn_3$  shows a broad structure at about 2 eV and a weak structure at about 3 eV. For  $CeSn_3$  the structure at about 2 eV becomes developed from the background and has small peaks at 1.8 and 2.3 eV. The structure at about 3 eV also becomes stronger.

Note that the magnitudes of the optical conductivities throughout this spectral region are quite different in both theoretical and experimental data.  $CeSn_3$  has one more electron per formula unit, the 4f electron. The conductivity sum rule difference in the 1.5–4.35 eV region between the two compounds in the experimental data is 1.18 electrons per formula unit, which can be stated as about 1, considering possible experimental errors [23]. Also, calculations based on a band model yield a conductivity that is larger for  $CeSn_3$  than for  $LaSn_3$ , giving a sum rule difference of 0.55 electrons per formula unit in the same energy region [23]. These results strongly indicate that the 4f states in  $CeSn_3$  are not so localized that the hybridization given by band theory plays an important role in explaining the low-energy optical property as well as the result of de Haas–van Alphen measurement for the compound [2].

## Acknowledgments

The author would like to thank Professor D W Lynch, Professor B N Harmon and Dr D D Koelling for helpful suggestions and discussions.

## References

- [1] Marabelli F and Wachter P 1987 *Phys. Rev. B* **36** 1238
- [2] Koelling D D 1982 *Solid State Commun.* **43** 247
- [3] Yanase A 1983 *J. Magn. Magn. Mater.* **31** 453
- [4] Johanson W R, Crabtree G W, Koelling D D, Edelstein A S and McMasters O D 1981 *J. Appl. Phys.* **52** 2134
- [5] Umehara I, Kurosawa Y, Nagai N, Kikuchi M, Satoh K and Onuki Y 1990 *J. Phys. Soc. Japan* **59** 2848
- [6] Hasegawa A, Yamagami H and Johbettoh H 1991 *J. Phys. Soc. Japan* **59** 2457  
Hasegawa A and Yamagami H 1991 *J. Phys. Soc. Japan* **60** 1654
- [7] Harris I R and Rayner G V 1965 *J. Less-Common Met.* **9** 7  
Cooper J R, Rizzuto C and Olcese G 1971 *J. Physique* **37** 1136
- [8] Tsuchida T and Wallace W E 1965 *J. Chem. Phys.* **43** 3811  
Malik S K, Vijayaragavan R, Greg S K and Ripmeester R J 1975 *Phys. Status Solidi b* **68** 399
- [9] Shenoy G K, Dunlap B D, Kalvius G M, Toxen A M and Gambino R J 1970 *J. Appl. Phys.* **41** 1317
- [10] Welsh L B, Toxen A M and Gambino R J 1971 *Phys. Rev. B* **4** 2921
- [11] Schoenes J 1982 *Valence Instabilities* ed P Wachter and H Boppart (Amsterdam: North-Holland) p 329
- [12] Marabelli F, Wachter P and Walker E 1989 *Phys. Rev. B* **39** 1407
- [13] Kwon Y S, Takeshige M, Suzuki T and Kasuya T 1990 *Physica B* **163** 328
- [14] van der Heide P A M, ten Cate H W, ten Dam L M, de Groot R A and de Vroomen A R 1986 *J. Phys. F: Met. Phys.* **16** 1617
- [15] Chen L-Y and Lynch D W 1987 *Appl. Opt.* **26** 5221
- [16] Koelling D D and Harmon B N 1977 *J. Phys. C: Solid State Phys.* **10** 3107
- [17] Gschneidner K A, Dhar S K, Stierman R J, Tsang T W E and McMasters O D 1985 *J. Magn. Mater.* **47-8** 51
- [18] Baer Y, Ott H R, Fuggle J C and de Long L E 1981 *Phys. Rev. B* **24** 5384
- [19] Hillebrecht F U, Fuggle J C, Sawatzky G A and Zeller R 1983 *Phys. Rev. Lett.* **51** 1187
- [20] Jepsen O and Anderson O K 1971 *Solid State Commun.* **9** 1763
- [21] Kim K J, Harmon B N and Lynch D W 1991 *Phys. Rev. B* **43** 1948
- [22] Koenig C and Khan M A 1988 *Phys. Rev. B* **38** 5887
- [23] Kim K J, Harmon B N, Lynch D W and Koelling D D 1991 *Phys. Rev. B* **44** 8526